

Interfacial thermal transport in atomic junctions

Lifa Zhang,¹ Pawel Keblinski,² Jian-Sheng Wang,¹ and Baowen Li^{3,1,*}

¹*Department of Physics and Centre for Computational Science and Engineering,
National University of Singapore, Singapore 117542, Republic of Singapore*

²*Department of Materials Science and Engineering,
Rensselaer Polytechnic Institute, New York, 12180, USA.*

³*NUS Graduate School for Integrative Sciences and Engineering, Singapore 117456, Republic of Singapore*

(Dated: 30 Oct 2010, Revised 10 Jan 2011)

We study ballistic interfacial thermal transport across atomic junctions. Exact expressions for phonon transmission coefficients are derived for thermal transport in one-junction and two-junction chains, and verified by numerical calculation based on a nonequilibrium Green's function method. For a single-junction case, we find that the phonon transmission coefficient typically decreases monotonically with increasing frequency. However, in the range between equal frequency spectrum and equal acoustic impedance, it increases first then decreases, which explains why the Kapitza resistance calculated from the acoustic mismatch model is far larger than the experimental values at low temperatures. The junction thermal conductance reaches a maximum when the interfacial coupling equals the harmonic average of the spring constants of the two semi-infinite chains. For three-dimensional junctions, in the weak coupling limit, we find that the conductance is proportional to the square of the interfacial coupling, while for intermediate coupling strength the conductance is approximately proportional to the interfacial coupling strength. For two-junction chains, the transmission coefficient oscillates with the frequency due to interference effects. The oscillations between the two envelop lines can be understood analytically, thus providing guidelines in designing phonon frequency filters.

PACS numbers: 66.70.-f, 05.60.-k, 44.10.+i,

I. INTRODUCTION

In the past decade there has been a significant research focus on thermal transport in micro scale¹. Several conceptual thermal devices, such as thermal rectifiers/diodes, thermal transistors, thermal logical gates, and thermal memory²⁻⁵, have been proposed, which, in principle, make it possible to control heat due to phonons and process information with phonons. The issue of quantum thermal transport in nanostructures was also addressed⁶. In this context, the critical information is in phonon transmission coefficients that in quasi-one-dimensional atomic models can be calculated by transfer matrix method⁷⁻¹⁰. However, the evaluation of the transfer matrix may be numerically unstable, particularly when the system size becomes large. Alternatively, nonequilibrium Green's function (NEGF) method is an efficient way to calculate the transmission coefficient¹¹. Unfortunately, both of these two methods are numerical in nature and do not give analytical expressions.

For thermal transport and control, the interfacial thermal scattering process is becoming increasingly important, especially in practical devices. Two theories, acoustic mismatch model²² and the diffuse mismatch model¹³, have been proposed to study the mechanism of the thermal interfacial resistance. However, both models offer limited accuracy in nanoscale interfacial resistance predictions¹⁴ because they neglect atomic details of actual interfaces. A scattering boundary method within the lattice dynamic approach was first proposed by Lumpkin and Saslow to study the Kapitza conductance in

a one-dimensional (1D) lattice¹⁵, and was then applied to calculate the Kapitza resistance in two- and three-dimensional (3D) lattices^{16,17}. This method can predict thermal interfacial conductance between heterogeneous materials with full consideration of the atomic structures in the interface. Recently, this method was applied to study the ballistic thermal transport in nanotube junctions¹⁸, spin chains¹⁹, and honeycomb lattice ribbons²⁰.

In this paper we give an explicit analytical expression of transmission coefficient obtained through the scattering boundary method, and use it to study the interfacial thermal transport across atomic junctions. First, in Sec. II, we introduce a model in which two semi-infinite 1D atomic chains are coupled either via a point junction or an extended junction region. By using the boundary scattering method we derive the exact expressions for phonon transmission coefficients for thermal transport in one-junction and two-junction chains in Sec. III. The role of various parameters on the junction conductance is analyzed and discussed in Sec. IV. In section IV we also estimate the interfacial conductance between two 3D solids. In Sec. V, we introduce briefly the NEGF method, and use it to verify the results from analytical formulae for the thermal transport in our model. A short summary is presented in Sec. VI.

II. MODEL

The one-dimensional atomic chain consists of three parts: two semi-infinite leads and an center region (see

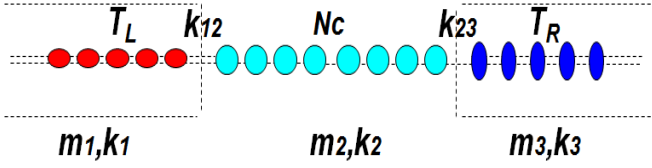


FIG. 1: (color online) A schematic representation of the 1D atomic chain model. The size of the center part is $N_C = 8$. The left and right regions are two semi-infinite harmonic atomic chains at different temperatures T_L and T_R . The three parts are coupled by harmonic springs with constant strength k_{12} and k_{23} ; all of which are harmonic chains with mass and spring constant as m_1, k_1 , m_2, k_2 and m_3, k_3 , respectively.

Fig. 1). The two leads are in equilibrium at different temperatures T_L and T_R . The three parts are coupled by harmonic springs with constant strength k_{12} and k_{23} ; all of which are harmonic chains with mass and spring constants m_1, k_1 , m_2, k_2 and m_3, k_3 , respectively. So the total Hamiltonian can be written as

$$H = \sum_{\alpha=1,2,3} H_{\alpha} + \frac{1}{2}k_{12}(x_{1,1} - x_{2,1})^2 + \frac{1}{2}k_{23}(x_{2,N_c} - x_{3,1})^2; \quad (1)$$

here,

$$H_{\alpha} = \sum_{i=1}^{N_{\alpha}} \frac{1}{2}m_{\alpha}\dot{x}_{\alpha,i}^2 + \sum_{i=1}^{N_{\alpha}-1} \frac{1}{2}k_{\alpha}(x_{\alpha,i} - x_{\alpha,i+1})^2. \quad (2)$$

Where $x_{\alpha,i}$ is the relative displacement of i -th atom in α -th part. If there is no center part, that is, the two semi-infinite leads connected directly by k_{12} , then by setting $\alpha = 1, 2$ and $k_{23} = 0$ in Eq. (1), we can obtain the corresponding Hamiltonian. For the semi-infinite leads, $N_{\alpha} = \infty$.

III. ANALYTICAL SOLUTION FROM THE SCATTERING BOUNDARY METHOD

Heat current flowing from left to right through a junction connecting two leads kept at different equilibrium heat-bath temperatures T_L and T_R is given by the Landauer formula⁶

$$I = \frac{1}{2\pi} \int_0^{\infty} \hbar\omega [f_L(\omega) - f_R(\omega)] T[\omega] d\omega, \quad (3)$$

which allows us to develop the junction conductance formula

$$\sigma = \frac{1}{2\pi} \int_0^{\infty} d\omega \hbar\omega T[\omega] \frac{\partial f(\omega)}{\partial T}, \quad (4)$$

here, $f_{L,R} = \{\exp[\hbar\omega/(k_B T_{L,R})] - 1\}^{-1}$ is the Bose-Einstein distribution for phonons, and $T[\omega]$ is the frequency dependent transmission coefficient. Therefore, the key step for the thermal transport characterization is to calculate the transmission coefficients.

We first consider a point-junction case, that is, two semi-infinite harmonic chains connected by a spring with constant strength k_{12} . We assume a wave solution transmitting from the left lead to the right lead. We label the atoms as $-\infty, \dots, -1, 0, 1, 2, \dots, +\infty$. Atoms 0 and 1 are connected by k_{12} spring. An incident wave from left is assumed as $x_I = \lambda_1^j e^{-i\omega t}$. When it arrives at the interface, it will be partially reflected and partially transmitted. The reflected wave amplitude is $x_R = r_{12} \lambda_1^{-j} e^{-i\omega t}$ and the transmission wave can be written as $x_T = t_{12} \lambda_2^{j-1} e^{-i\omega t}$. So at each atom we have $\dots, x_{-1} = (\lambda_1^{-1} + r_{12} \lambda_1) e^{-i\omega t}$, $x_0 = (1 + r_{12}) e^{-i\omega t}$, $x_1 = t_{12} e^{-i\omega t}$, $x_2 = t_{12} \lambda_2 e^{-i\omega t}$, \dots . Here, $\lambda_j = e^{iq_j a_j}$, q_j is the wave vector, a_j is the interatomic spacing. For the atom in the j -th part, we can have the equation of motion as

$$m_j \frac{d^2 x_{j,n}}{dt^2} = k_j (x_{j,n+1} - x_{j,n}) + k_j (x_{j,n} - x_{j,n-1}), \quad (5)$$

each wave transport separately and satisfies such equation. Thus λ_j satisfies the dispersion relation of the corresponding lead as

$$\omega^2 m_j = -k_j \lambda_j^{-1} + 2k_j - k_j \lambda_j. \quad (6)$$

The quadratic equation has two roots. Which one should we choose? Replacing ω with $\omega + i\eta$, $\eta = 0^+$, none of the eigenvalues λ will have modulus exactly 1. We find for the traveling waves²¹

$$|\lambda| = 1 - \eta \frac{a}{v}, \quad (7)$$

thus the forward moving waves with group velocity $v > 0$ have $|\lambda| < 1$. Therefore we should take the one with $|\lambda| < 1$ of the two roots which are given as

$$\lambda_j = \frac{-h_j \pm \sqrt{h_j^2 - 4}}{2}, \quad h_j = \frac{m_j}{k_j} (\omega + i\eta)^2 - 2. \quad (8)$$

From the scattering boundary method, the coefficients r_{12}, t_{12} can be obtained from the continuity condition at the interface as:

$$\omega^2 m_1 x_0 = -k_1 x_{-1} + (k_1 + k_{12}) x_0 - k_{12} x_1; \quad (9)$$

$$\omega^2 m_2 x_1 = -k_{12} x_0 + (k_{12} + k_2) x_1 - k_{12} x_2. \quad (10)$$

Finally we can get the transmission coefficient as

$$T[\omega] = 1 - |r_{12}|^2 = 1 - |r_{21}|^2, \quad (11)$$

here,

$$r_{ij} = \frac{k_i (\lambda_i - 1/\lambda_i) (k_j - k_{ij} - k_j/\lambda_j)}{(k_i - k_{ij} - k_i/\lambda_i) (k_j - k_{ij} - k_j/\lambda_j) - k_{ij}^2} - 1. \quad (12)$$

Of course, we can also use t_{12} to express $T[\omega]$ as $\frac{m_2 v_2 / a_2}{m_1 v_1 / a_1} |t_{12}|^2$, here the group velocity $v_i = \frac{d\omega}{dq_i} =$

$\frac{a_i}{2} \sqrt{\frac{4k_i}{m_i} - \omega^2}$, which is derived from the dispersion relation given by Eq. (6). Thus, the transmission coefficient can also be expressed as

$$T[\omega] = \frac{\sqrt{4k_2 m_2 - \omega^2 m_2^2}}{\sqrt{4k_1 m_1 - \omega^2 m_1^2}} |t_{12}|^2, \quad (13)$$

here

$$t_{ij} = \frac{-k_{ij} k_i (\lambda_i - 1/\lambda_i)}{(k_i - k_{ij} - k_i/\lambda_i)(k_j - k_{ij} - k_j/\lambda_j) - k_{ij}^2}. \quad (14)$$

For the long-wave limit, that is, $\omega = 0^+$, we get $r_{ij} = \frac{\sqrt{k_i m_i} - \sqrt{k_j m_j}}{\sqrt{k_i m_i} + \sqrt{k_j m_j}}$; and the transmission is

$$T[0^+] = \frac{4\sqrt{k_1 m_1 k_2 m_2}}{(\sqrt{k_1 m_1} + \sqrt{k_2 m_2})^2}. \quad (15)$$

This result is consistent with the one obtained for the acoustic mismatch model, i.e., $T = \frac{4Z_1 Z_2}{(Z_1 + Z_2)^2}$.²² Where the acoustic impedance is $Z_i = \rho_i v_i = (m_i/a_i)v_i$, and $Z_i(\omega = 0^+) = \sqrt{k_i m_i}$. We note that in acoustic mismatch model the transmission coefficient is frequency independent, and in reality it only applies in the limit of low frequency/long wavelengths. In this case the phonon sees the interface only as a discontinuity between two semi-infinite media and the transmission does not depend on the coupling spring strength k_{ij} . If the two leads have the same acoustic impedance for long wave limit, then $T[0^+] = 1$; otherwise $T[0^+] < 1$.

For a two-junction case, which is shown in Fig. 1, the transmission wave will be reflected and transmitted by the second boundary, leading to multiple reflections. Finally the total transmitted wave function is obtained as a superposition of multiple reflections and transmissions, resulting in the transmission coefficient through the center part

$$T[\omega] = \frac{(1 - |r_{12}|^2)(1 - |r_{23}|^2)}{|1 - r_{23} r_{21} \lambda_2^{2(N_C-1)}|^2}, \quad (16)$$

here r_{ij} and λ_i are determined by Eq. (12) and Eq. (8); N_C is the number of atoms in the center atomic chain. From this expression, we can find that the transmission coefficient oscillates with frequency, and is between the envelope lines of maximum and minimum transmission, which are $T_{\max}[\omega] = (1 - |r_{12}|^2)(1 - |r_{23}|^2)/(1 - |r_{23} r_{21}|)^2$ for constructive interference and $T_{\min}[\omega] = (1 - |r_{12}|^2)(1 - |r_{23}|^2)/(1 + |r_{23} r_{21}|)^2$ for destructive interference.

IV. RESULTS AND DISCUSSIONS

A. Thermal transport in 1D one-junction chains

In Sec. III, we have derived the analytical expressions for the phonon transmission coefficient for point-junction and extended-junction (two point junction)

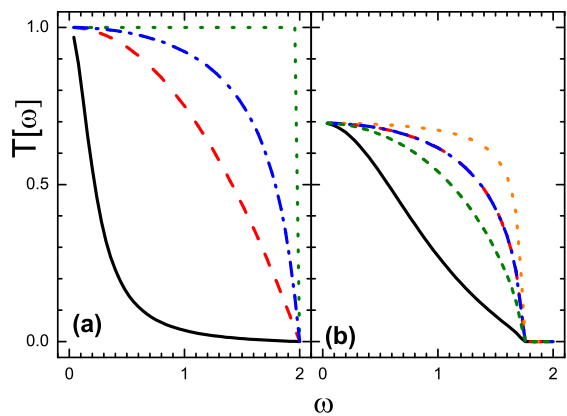


FIG. 2: (color online) The transmission coefficient vs frequency ω for different interface coupling k_{12} in one-junction chains. (a) shows the transmission in one junction connected by the same semi-infinite atomic chains with $k_1 = k_2 = 1.0$, $m_1 = m_2 = 1.0$; the solid, dashed, dotted and dash-dotted lines correspond to $k_{12} = 0.1, 0.5, 1.0$ and 2.0 , respectively. (b) shows the transmission in one junction connected by two different semi-infinite atomic chains with $k_1 = 1.0$, $m_1 = 1.0$, $k_2 = 3.0$ and $m_2 = 4.0$; the solid, dashed, dotted, dash-dotted and shot-dashed lines correspond to $k_{12} = 0.5, 1.0, 1.5, 3.0$ and 8.0 , respectively.

cases Eq. (11), Eq. (12) and Eq. (16) by using the scattering boundary method. Using these analytical expressions, we analyze the role of various parameters on the thermal transport in one- and two-point junctions.

Figure 2 shows the transmission coefficient as a function of frequency for a different interface spring constant k_{12} for the point-junction model. The maximum frequency at which the transmission coefficient is above zero is equal to the minimum of $2\sqrt{k_1/m_1}$ and $2\sqrt{k_2/m_2}$. In Fig. 2(a), the two semi-infinite atomic chains have the same mass and spring constant. When the inter-

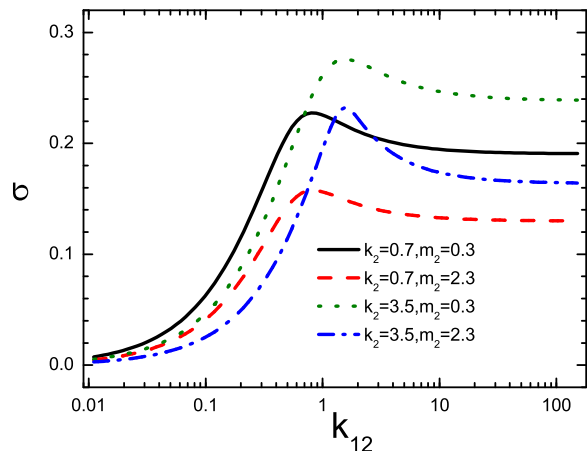


FIG. 3: (color online) The thermal conductance vs interface coupling k_{12} in point-junction model. Here, $k_1 = 1.0$, $m_1 = 1.0$.

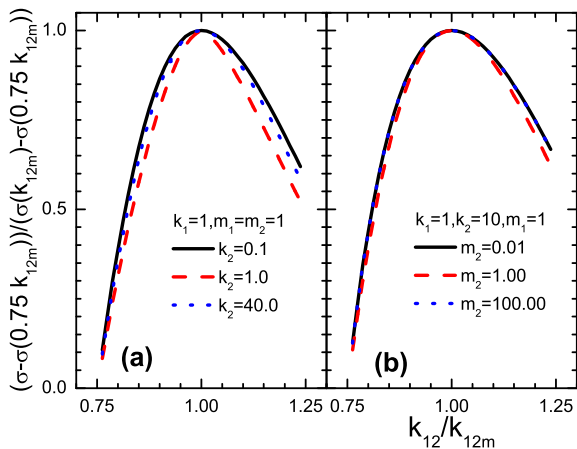


FIG. 4: (color online) The thermal conductance vs the ratio of k_{12}/k_{12m} in one-junction atomic chain. Here k_{12m} is the harmonic average of the spring constants of the two semi-infinite leads. (a) $k_1 = 1.0$, $m_1 = m_2 = 1.0$; the solid, dashed, and dotted lines correspond to $k_2 = 0.1$, 1.0 , and 40.0 , respectively. (b) $k_1 = 1.0$, $m_1 = 1.0$, $k_2 = 10.0$; the solid, dashed, and dotted lines correspond to $m_2 = 0.01$, 1.0 , and 100.0 , respectively.

face coupling k_{12} equals to that of the chains, the transmission is equal to one in the whole frequency domain, because of the homogeneity of the chain structure. If k_{12} increases or decreases, the transmission coefficient decreases. If we set $k_1/m_1 = k_2/m_2$, the transmission coefficient exhibits similar behavior, the only difference is that the transmission coefficient changes to the value obtained by Eq. (15). In Fig. 2(b), the two semi-infinite atomic chains have different masses and spring constants. The transmission decreases with increased frequency for all the coupling values k_{12} . Also, it appears that for a given frequency the transmission is maximized for a k_{12} value residing between k_1 and k_2 . From Eq. (11) and Eq. (12), $T[\omega] = 0$, if $k_{12} = 0$; and $T[\omega]$ has definite value $1 - \left| \frac{k_1(\lambda_1 - 1) - k_2(1 - \lambda_2^{-1})}{k_1(1 - \lambda_1^{-1}) + k_2(1 - \lambda_2^{-1})} \right|^2$, if $k_{12} = \infty$.

The maximum transmission concept results in the maximum junction conductance as shown in Fig. 3. With the increasing of k_{12} , we find that the conductance will first increase, then arrive at maximum value, and then slightly decrease and at last it will tend to a constant. We find that the maximum transmission or conductance occurs at k_{12} given by

$$k_{12} = k_{12m} = \frac{2k_1k_2}{k_1 + k_2}, \quad (17)$$

i.e., when the coupling spring stiffness is equal to the harmonic average of spring connecting atoms in the two semi-infinite chains. In Fig. 4, we show the thermal conductance vs the ratio of k_{12} and k_{12m} . For the two semi-infinite chains with the same mass $m_1 = m_2$, the maximum conductance occurs exactly at k_{12m} . If the two leads have different masses $m_1 \neq m_2$, the maximum con-

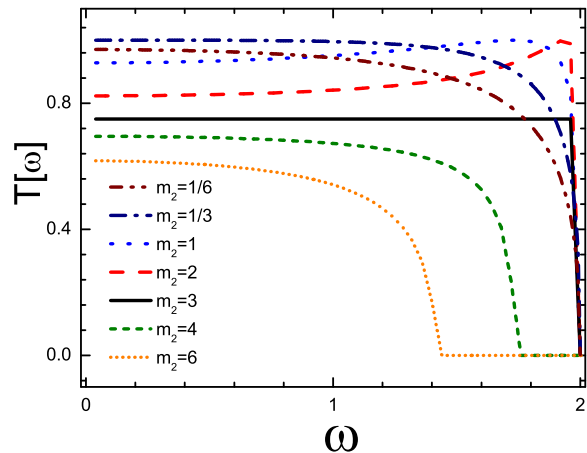


FIG. 5: (color online) The transmission coefficient vs frequency for different mass ratios m_2/m_1 at the interface coupling k_{12m} . Here, $k_1 = 1.0$, $k_2 = 3.0$, $k_{12} = k_{12m} = 1.5$ and $m_1 = 1.0$.

ductance is almost exactly at the k_{12m} point, for mass ratios ranging from 0.01 to 100.

In Fig. 5, we show the curves of the transmission as a function of frequency for interface coupling equal to k_{12m} . If $k_1/m_1 = k_2/m_2$, that is, when both chains have the same frequency spectrum of $[0, 2\sqrt{k_1/m_1}]$, the transmission equals to a constant $T[\omega] = T[0^+]$, which can be seen from the solid line in Fig. 5, and which is consistent with Fig. 2(a). Thus for chains with matched spectra the transmission is frequency independent. Let us now fix k_1, k_2 and k_2 , and decrease m_2 . In the range between the point of equal-spectrum ($\omega_m = k_1/m_1 = k_2/m_2$) and the one of equal-impedance ($Z(\omega = 0^+) = k_1m_1 = k_2m_2$), the transmission will first increase with frequency and then decrease. Otherwise, there is a monotonic decrease. The former behavior is quite interesting, as one

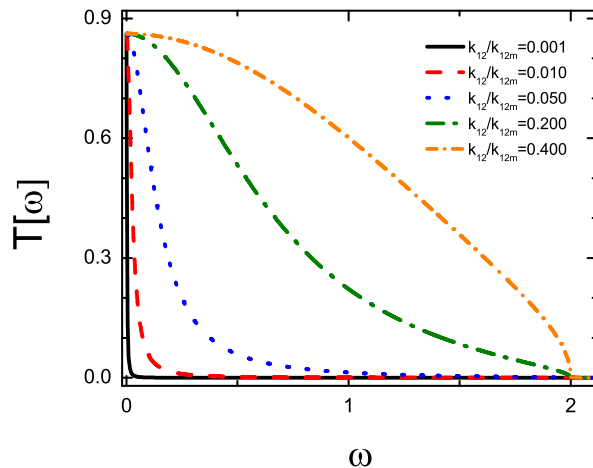


FIG. 6: (color online) The transmission coefficient vs frequency for different interface coupling k_{12m} . Here, $k_1 = 1.0$, $m_1 = 1.0$, $k_2 = 0.7$, $m_2 = 0.3$.

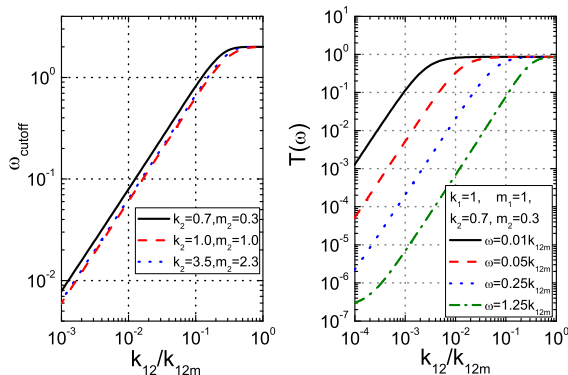


FIG. 7: (color online) (a) The cutoff frequency vs interface coupling for 1D one-junction atomic chains. The parameters are: $k_1 = 1.0$, $m_1 = 1.0$. (b) The transmission as function of interface coupling for 1D one-junction atomic chains. The parameters are: $k_1 = 1.0$, $m_1 = 1.0$, $k_2 = 0.7$, $m_2 = 0.3$

expects that the transmission should be the largest in the long wavelength limit. For highly dissimilar materials, the transmission coefficient in the whole frequency range is much larger than that in the long wave limit $T[\omega = 0^+] = \frac{4Z_1Z_2}{(Z_1+Z_2)^2}$, thus the real conductance is far larger than that calculated from the acoustic mismatch model. This result explain why the interfacial resistance calculated from the acoustic mismatch model is far larger than the experimental value measured at low temperatures, where the phonon transport can be regarded as ballistic transport.

In many real interfaces, interface coupling is very weak, that is, the k_{12} is less than k_{12m} . So it is desirable to study the thermal transport in atomic chains in the weak coupling limit. Figure 6 shows the transmission coefficient as function of interface coupling. In the weak coupling limit, with the frequency increasing, the transmission decreases rapidly to zero, so the frequency region where phonons are effectively transmitted is very narrow. With interface strength increasing, more and more modes contribute to the transmission and the phonon transmission window widens. If the interface coupling increases further, that is $k_{12}/k_{12m} > 0.1$, out of the weak interface coupling limit, all the phonons contribute to the transmission. The only further change with increasing k_{12} is the actual values of the transmission coefficients increase. In Fig. 7(a), we show the transmission cutoff frequency as function of the interface coupling. Here, we define the cutoff frequency ω_{cutoff} at which the transmission $T(\omega_{\text{cutoff}}) = 0.1T(0^+)$. We find that the cutoff frequency shows linear dependance on interface coupling in the weak coupling limit $k_{12} < 0.1k_{12m}$. If the interface strength increase further, the cutoff frequency is saturated. In Fig. 7(b), we show the transmission as function of interface coupling for several different phonons. We find that in the weak interface coupling region, the transmission is proportional to the square of the interface coupling, which is consistent with the formulas Eq. (13)

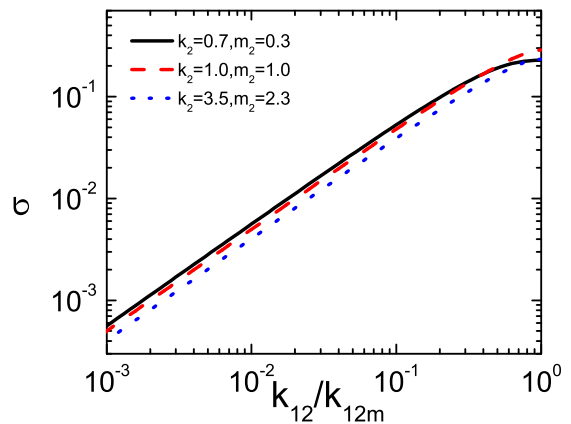


FIG. 8: (color online) The thermal conductance vs interface coupling for 1D point-junction atomic chains. The parameters are: $k_1 = 1.0$, $m_1 = 1.0$.

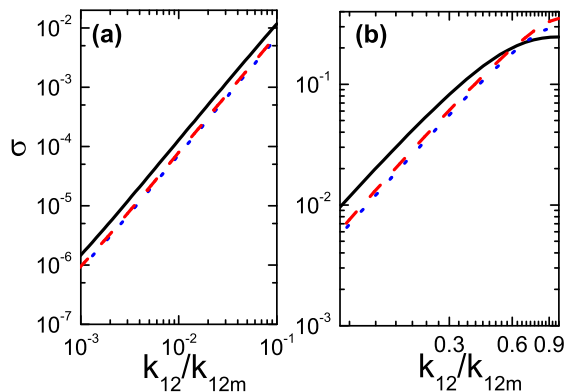


FIG. 9: (color online) The thermal conductance vs interface coupling for 3D one-junction atomic chains. The parameters are the same with Fig. 8. (a) Interface coupling is far less than the coupling k_{12m} : $k_{12m}/k_{12} = 0.001 - 0.1$; (b) Interface coupling is in the region of $0.1k_{12m} \sim 0.9k_{12m}$.

and Eq. (14). In the weak interface coupling region, for the 1D atomic one-junction chains, it is shown that the thermal conductance is linear with the interface coupling (see Fig. 8). If we strengthen the interface coupling between the two chains, the conductance will be linearly enhanced. For different mismatched chains, the absolute values of the conductance are different, but dependence on the coupling strength is the same.

B. Thermal transport in 3D single-interface structures

The thermal conductance Eq. (4) can also be written as²³:

$$\sigma = \int_0^\infty d\omega \hbar\omega T[\omega] \frac{\partial f(\omega)}{\partial T} v(\omega) D(\omega), \quad (18)$$

because of $v(\omega) = \partial\omega/\partial k$ and phonon density of states

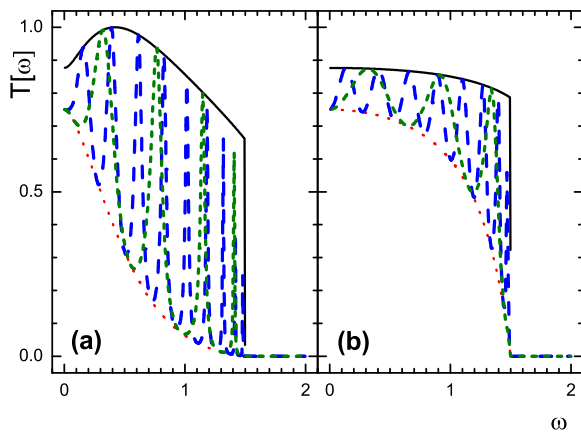


FIG. 10: (color online) The transmission coefficient of the two-junction atomic chains. Parameters: $k_1 = 1.0$, $m_1 = 1.0$, $k_2 = 0.9$, $m_2 = 1.6$, $k_3 = 4.5$, $m_3 = 2.0$. The solid, dotted, dashed and shot dashed lines correspond to maximum transmission, minimum transmission, $N_c = 4$ and $N_c = 9$, respectively. The interface couplings are different: (a) $k_{12} = 0.3$, $k_{23} = 0.7$; (b) $k_{12} = 1.0$, $k_{23} = 4.5$.

in 1D structure, $D(\omega) = 1/(2\pi v)$, we can obtain Eq. (4). In order to estimate the behavior of the interfacial thermal transport across interfaces in 3D structures, we only need to change the phonon density of states in the above equation. Because the density of states for 3D structure within the Debye approximation is $D(\omega) \sim \omega^2$, therefore we can replace ω with ω^3 in Eq. (4); the thermal conductance as a function of the coupling strength is shown in Fig. 9. From Fig. 9(a), we find that in the weak interface limit, conductance is proportional to the square of interface coupling, which is consistent with the results from other models^{24–26}, while it is linear dependent on the interface coupling in 1D junctions. This is due to the fact that in 3D low frequency region contributes relatively little to the conductance as the density of states is low there. If the interface coupling increases further, that is $k_{12}/k_{12m} > 0.1$, out of the weak interface coupling limit, all the modes contribute to the transmittance, the conductance is no longer proportional to the square of the interface coupling, and the slope continuously decreases. In some intermediate ranges the conductance is approximately proportional to the interfacial coupling (see Fig. 9(b)), which is consistent with the results from molecular simulation approach²⁷. For stronger coupling the conductances for the 1D case and 3D one have similar behaviors, the slope of both cases will decrease continuously to be zero at point k_{12m} , where the conductance will be maximized and then decrease slightly to a limiting value.

C. Thermal transport in extended junctions

Now we focus on a case where the junction is extended and involves a center part. The overall behavior of the

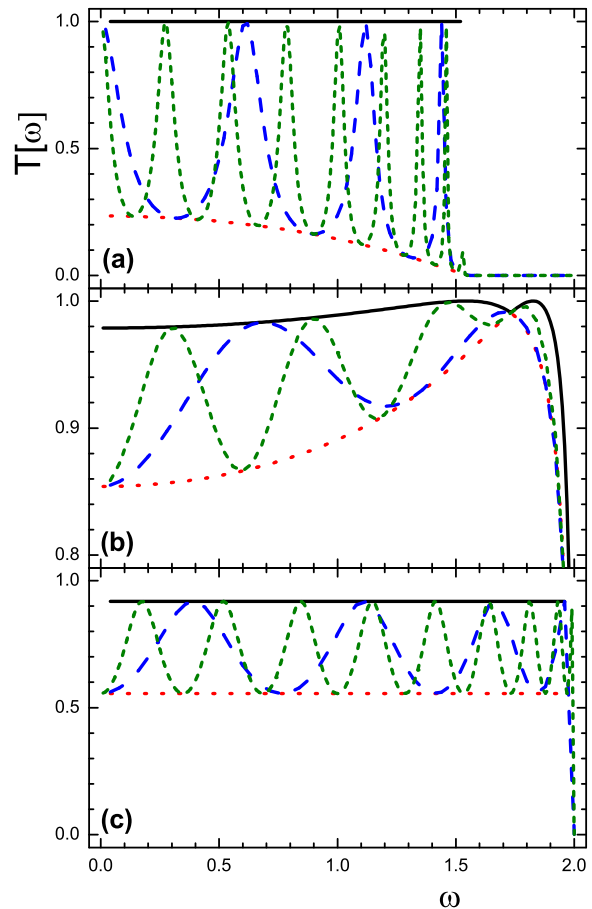


FIG. 11: (color online) The transmission coefficient of the two-junction atomic chains. Here, $k_1 = 1.0$, $m_1 = 1.0$. The solid, dotted, dashed and shot dashed lines correspond to maximum transmission, minimum transmission, $N_c = 4$ and $N_c = 9$, respectively. (a) $k_2 = 3.0$, $m_2 = 5.0$, $k_3 = 1.0$, $m_3 = 1.0$, $k_{12} = k_{23} = 1.0$; (b) $k_2 = 3.0$, $m_2 = 1.0$, $k_3 = 5.0$, $m_3 = 1.0$, $k_{12} = k_{12m} = 1.5$, $k_{23} = k_{23m} = 3.75$; (c) $k_2 = 3.0$, $m_2 = 3.0$, $k_3 = 5.0$, $m_3 = 5.0$, $k_{12} = k_{12m} = 1.5$, $k_{23} = k_{23m} = 3.75$.

transmission is the combination of the transmission behavior in single point-junction case and the oscillatory behavior due to phonon interferences arising from multiple scattering. We show the transmission coefficient as a function of frequency of an arbitrary case in Fig. 10(a). Here, the three chain parts have different masses and spring constants, and the interface coupling is not special. From the analytical expression of Eq. (16), we plot curves of the maximum transmission and minimum transmission, $N_c = 4$ and $N_c = 9$. The transmission oscillates between the envelop lines of maximum and minimum transmission. The maximum transmission line will increase first, and the minimum transmission line will monotonically decrease with frequency. However for interface coupling that is the same with the leads, the two envelop lines will monotonically decrease, which can be seen in Fig. 10(b).

For some special cases, the transmission coefficient in

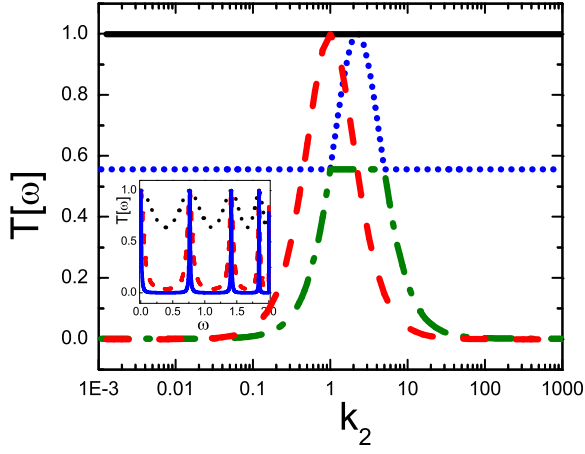


FIG. 12: (color online) The maximum and minimum transmission coefficient of the two-junction atomic chains. Here, $k_1 = 1.0$, $m_1 = 1.0$. The solid, dashed lines correspond to maximum transmission and minimum transmission $k_3 = 1.0$, $m_3 = 1.0$, respectively; the dotted and dash-dotted lines correspond to maximum transmission and minimum transmission $k_3 = 5.0$, $m_3 = 5.0$, respectively. The inset shows the transmission coefficient with frequency for different k_2 . $k_1 = k_3 = 1.0$, $m_1 = m_3 = 1.0$. The dotted, dashed, and solid lines correspond to $k_2 = 0.5, 0.1$, and 0.02 respectively. For all the curves, $m_2 = k_2$ and $k_{12} = k_{12m}$, $k_{23} = k_{23m}$.

the frequency domain has interesting phenomena, which are shown in Fig. 11. In Fig. 11(a), the transmission for the case of two identical leads is shown. In this case, the maximum transmission is equal to one, the infinite-long wavelength phonon and the resonance mode can transmit fully through the center part. The minimum transmission is very low, indicating efficient destructive interference. Figure 11(b) shows the transmission when all three parts are different and connected by interface couplings k_{12m} and k_{23m} . We find that overall trend for the maximum and minimum transmission lines is increasing first, then decreasing. If, in addition, the ratios of k_i/m_i are the same for three parts, then the maximum and minimum transmission are constants in the whole frequency range, and the transmission coefficient through finite-size center part oscillate between the two constants, which can be clearly seen in Fig. 11(c). Therefore, we can use the above properties of transmission to design the frequency filters. Figure 12 shows the maximum and minimum transmission coefficient for the filter. If the spring constant of the center part is very different from the ones of the the two leads, the oscillatory peak is sharp, and transmission for most of the frequency will tend to zero, only few resonant frequency can be transmitted. This finding provides guidelines for the design of selective frequency filters.

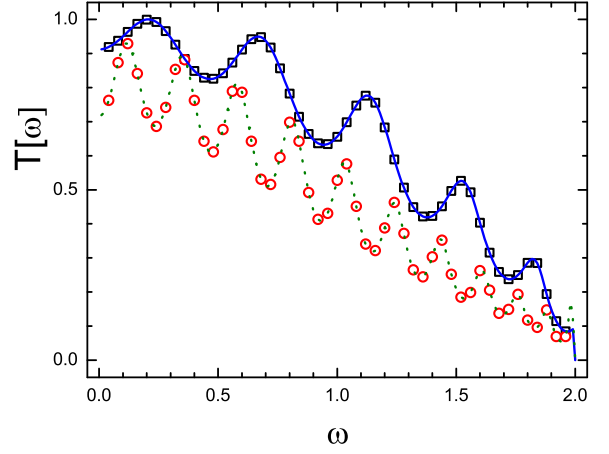


FIG. 13: (color online) The comparison of the results from scattering boundary method and nonequilibrium Green's function method for the transmission coefficient in two-junction atomic chains. The square curve and solid line correspond the parameters: $N_c = 6$, $k_1 = 1.0$, $m_1 = 1.0$, $k_2 = 1.5$, $m_2 = 1.3$, $k_3 = 2.0$, $m_3 = 1.7$, $k_{12} = 1.3$, $k_{23} = 0.8$; the circle curve and dashed line correspond the parameters: $N_c = 13$, $k_1 = 1.0$, $m_1 = 1.0$, $k_2 = 1.5$, $m_2 = 1.3$, $k_3 = 4.0$, $m_3 = 2.7$, $k_{12} = 1.3$, $k_{23} = 0.8$. The square and circle curves are the results from nonequilibrium Green's function method; The solid and dash lines are the results from scattering boundary method.

V. VERIFICATION BY NONEQUILIBRIUM GREEN'S FUNCTION METHOD

The NEGF method is an exact approach to study the ballistic thermal transport through junctions. Following the discussion in Sec. II, if we use a transformation for the coordinates, $u_j = \sqrt{m_j}x_j$, which is called the mass-normalized displacement, then the Hamiltonian can be written as

$$H = \sum_{\alpha=1,2,3} H_{\alpha} + \sum_{\beta=1,3} U_{\beta}^T V_{\beta,2} U_2, \quad (19)$$

where $H_{\alpha} = \frac{1}{2} (P_{\alpha}^T P_{\alpha} + U_{\alpha}^T K_{\alpha} U_{\alpha})$. K_{α} is the mass-normalized spring constant matrix, and $V_{12} = (V_{21})^T$ is the coupling matrix of the left lead to the central region and similarly for V_{23} is the coupling matrix of the right lead to the central region. As stated in Ref.⁷, the element of the coupling matrix $V_{\alpha,\beta}^{ij}$ is equal to $-k_{ij}/\sqrt{m_i m_j}$ which corresponding to the coupling between the i_{th} atom in region α and the j_{th} atom in region β .

We can use the nonequilibrium Green's function method⁶ to study the thermal transport in the atomic chain. We define the contour-ordered Green's function as

$$G^{\alpha\beta}(\tau, \tau') \equiv -\frac{i}{\hbar} \langle \mathcal{T} U_{\alpha}(\tau) U_{\beta}(\tau')^T \rangle, \quad (20)$$

where α and β refer to the region that the coordinates belong to and \mathcal{T} is the contour-ordering operator. Then

the equations of motion of the Green's function can be derived. In particular, the retarded Green's function for the central region in frequency domain is

$$G^r[\omega] = \left[(\omega + i\eta)^2 - K_2 - \Sigma^r[\omega] \right]^{-1}. \quad (21)$$

Here, $\Sigma^r = \sum_{\alpha=1,3} \Sigma_{\alpha}^r$, and $\Sigma_{\alpha} = V_{2,\alpha} g_{\alpha} V_{\alpha,2}$ is the self-energy due to interaction with the heat bath, $g_{\alpha}^r = [(\omega + i\eta)^2 - K_{\alpha}]^{-1}$. And in the advanced Green's function $G^a = (G^r)^{\dagger}$, the transmission coefficient can be calculated by the so-called Caroli formula as

$$T_{\beta\alpha}[\omega] = \text{Tr}(G^r \Gamma_{\beta} G^a \Gamma_{\alpha}), \quad (22)$$

where $\Gamma_{\alpha} = i(\Sigma_{\alpha}^r[\omega] - \Sigma_{\alpha}^a[\omega])$.

For single-junction atomic chains, if we regard the two atoms in the interface (atom 0 and atom 1) as the center part, then we can still use the formulae above to study the phonon transmission leading to the exact formula yielding the same result with the one obtained from the scattering boundary method. In Appendix A, We give the analytical proof of this fact.

For two-junction atomic chains, according to the NEGF formulas, we do the numerical calculation and plot the curves of the transmission coefficient as a function of frequency and compare them to the results obtained the scattering boundary method (see Fig. 13). We find that for any arbitrary case, the results from the NEGF method and the scattering boundary method are exactly the same. If there is no many-body interaction, that is, for the ballistic thermal transport the scattering matrix approach and the Green's function method give the same results. These two methods are equivalent, which has been proved from other points of view in Refs.^{28,29}.

VI. CONCLUSION

In this paper, we study the ballistic interfacial thermal transport in atomic junctions, we give the analytical simple formulae Eq. (11), Eq. (12) and Eq. (16) for the transmission of one-junction and two-junction cases, which are consistent with the results from the NEGF method.

For one-junction case, we find the transmission and conductance are maximized when the interface spring constant equals to the harmonic average of the two spring

constants of the leads. At the point near $k_{12} = k_{12m}$, the transmission $T[\omega]$ is a constant if $k_2/m_2 = k_1/m_1$; if not equal, in the range between $k_1/m_1 = k_2/m_2$ and $k_1 m_1 = k_2 m_2$, the transmission coefficient increases first then decreases with the increasing of frequency, otherwise the transmission monotonically decreases as the frequency increasing. For weak interface coupling, the cutoff frequency and the interface conductance for 1D chain is linear dependent with the interface coupling strength.

Because of different density of states, we change the formula of conductance to mimic the thermal transport in 3D junctions. In weak interface coupling limit, we find that the conductance is proportional to the square of the interface coupling, which is consistent with the results from other models. The slope of the conductance as function of interfacial coupling strength decreases continuously from two to zero, in certain range of which, the conductance is linear proportional to the interface coupling, which are consistent with the results of other molecular simulations.

For two-junction case, the transmission will oscillate with frequency in the envelop lines of maximum and minimum transmission which are determined by the one-junction picture. The transmission sometimes oscillates between two decreasing envelop lines, sometimes between two increasing envelop curves, or between two constants, etc.

Acknowledgements

P. K. is supported by the U.S. Air Force Office of Scientific Research Grant No. MURI FA9550-08-1-0407. J.-S. W. acknowledge support from a NUS research grant R-144-000-257-112.

Appendix A: Analytical proof of the equality of the two methods for one junction

In this appendix we give the analytical proof for the equality of the scattering boundary method and the non-equilibrium Green's function approach for the one-junction atomic chains.

From the scattering boundary method, we obtain the transmission Eq. (13) and Eq. (14), that is

$$T[\omega] = \frac{\sqrt{4k_2 m_2 - \omega^2 m_2^2}}{\sqrt{4k_1 m_1 - \omega^2 m_1^2}} \left| \frac{-k_{12} k_1 (\lambda_1 - 1/\lambda_1)}{(k_1 - k_{12} - k_1/\lambda_1)(k_2 - k_{12} - k_2/\lambda_2) - k_{12}^2} \right|^2, \quad (A1)$$

From the dispersion relation Eq. (6), we can obtain

$$k_j - k_j/\lambda_j = \omega^2 m_j - k_j(1 - \lambda_j) \quad (A2)$$

; and

$$k_j^2 |\lambda_j - 1/\lambda_j|^2 = \omega^2 (4k_j m_j - \omega^2 m_j^2) \quad (A3)$$

, So we can get

$$T[\omega] = \frac{k_{12}^2 \omega^2 \sqrt{4k_1 m_1 - \omega^2 m_1^2} \sqrt{4k_2 m_2 - \omega^2 m_2^2}}{[\omega^2 m_1 - k_1(1 - \lambda_1) - k_{12}][\omega^2 m_2 - k_2(1 - \lambda_2) - k_{12}] - k_{12}^2}. \quad (\text{A4})$$

Using the NEGF formulae, we regard the two atoms in the interface (atom 0 and atom 1) as the center part 0, then the dynamic matrix of the center as

$$K_0 = \begin{pmatrix} \frac{k_1 + k_{12}}{m_1} & \frac{-k_{12}}{\sqrt{m_1 m_2}} \\ \frac{-k_{12}}{\sqrt{m_1 m_2}} & \frac{k_{12} + k_2}{m_1} \end{pmatrix}. \quad (\text{A5})$$

And the coupling matrices between the leads (parts 1 and 2) and the center (part 0) are $V_{01} = (k_1/m_1, 0)^T$ and $V_{02} = (0, k_2/m_2)^T$, and according to Ref.³⁰, we can obtain the surface Green's function as

$$g_i^r = -\frac{m_i \lambda_i}{k_i}, \quad (\text{A6})$$

here, $i = 1, 2$ corresponds to the left and right lead. Then we can get the self energy ($\Sigma^r = V_{01} g_1^r V_{10} + V_{02} g_2^r V_{20}$) as

$$\Sigma^r = \begin{pmatrix} -\frac{k_1 \lambda_1}{m_1} & 0 \\ 0 & -\frac{k_2 \lambda_2}{m_2} \end{pmatrix}. \quad (\text{A7})$$

Thus we can calculate the retarded Green's function of the center $G^r = (\omega^2 I - K_0 - \Sigma^r)^{-1}$, which reads as

$$G^r = \begin{pmatrix} A_1 & B \\ B & A_2 \end{pmatrix}^{-1} = \frac{1}{\Delta} \begin{pmatrix} A_2 & -B \\ -B & A_1 \end{pmatrix}, \quad (\text{A8})$$

here, I is two-dimensional identity matrix and

$$A_i = \omega^2 - \frac{k_i}{m_i}(1 - \lambda_i) - \frac{k_{12}}{m_i}; \quad (\text{A9})$$

$$B = \frac{k_{12}}{\sqrt{m_1 m_2}}; \Delta = A_1 A_2 - B^2. \quad (\text{A10})$$

The advanced Green's function G^a equals to $(G^r)^\dagger$. And from the self energy we can get

$$\Gamma_1 = \begin{pmatrix} C_1 & 0 \\ 0 & 0 \end{pmatrix}; \Gamma_2 = \begin{pmatrix} 0 & 0 \\ 0 & C_2 \end{pmatrix}, \quad (\text{A11})$$

here, $C_i = \frac{\omega}{m_i} \sqrt{4k_i m_i - \omega^2 m_i^2}$. Therefore, we can calculate the transmission coefficient from the Caroli formula Eq. (22), at last we obtain

$$T[\omega] = Tr(G^r \Gamma_1 G^a \Gamma_2) = \frac{B^2 C_1 C_2}{\Delta \Delta^*} = \frac{B^2 C_1 C_2}{|A_1 A_2 - B^2|^2} \quad (\text{A12})$$

Inserting the values of A_i, B and C_i , we get exactly the same result with Eq. (A4). Therefore, the results from the scattering boundary method and non-equilibrium Green's function approach are equivalent.

* Electronic address: phylibw@nus.edu.sg

- ¹ A Dhar, Adv. Phys. **57**, 457 (2008).
- ² M. Terraneo, M. Peyrard, and G. Casati, Phys. Rev. Lett. **88**, 094302 (2002); B. Li, L. Wang, and G. Casati, Phys. Rev. Lett. **93**, 184301 (2004); D. Segal and A. Nitzan, Phys. Rev. Lett. **94**, 034301 (2005); C. W. Chang, D. Okawa, A. Majumdar, and A. Zettl, Science **314**, 1121 (2006).
- ³ B. Li, L. Wang, and G. Casati, Appl. Phys. Lett. **88**, 143501 (2006).
- ⁴ L. Wang and B. Li, Phys. Rev. Lett. **99**, 177208 (2007).
- ⁵ L. Wang and B. Li, Phys. Rev. Lett. **101**, 267203 (2008).
- ⁶ J.-S. Wang, J. Wang, and J. T. Lü, Eur. Phys. J. B **62**, 381 (2008).
- ⁷ P. Tong, B. Li, and B. Hu, Phys. Rev. B **59**, 8639 (1999).
- ⁸ E. Maciá, Phys. Rev. B **61**, 6645 (2000).
- ⁹ L. S. Cao, R. W. Peng, R. L. Zhang, X. F. Zhang, Mu Wang, X. Q. Huang, A. Hu, and S. S. Jiang, Phys. Rev. B **72**, 214301 (2005).
- ¹⁰ V. B. Antonyuk, M. Larsson, A. G. Malshukov, and K. A.

Chao, Semicond. Sci. Technol. **20**, 347 (2005).

- ¹¹ H. Haug and A. P. Jauho, *Quantum Kinetics in Transport and Optics of Semiconductors* (Springer, 1996); J.-S. Wang, J. Wang, and N. Zeng, Phys. Rev. B **74**, 033408 (2006); L. Zhang, J. -S. Wang, and B. Li, New J. Phys. **11**, 113038 (2009).
- ¹² W. Little, Can. J. Phys. **37**, 334 (1959).
- ¹³ E. Swartz and R. Pohl, Rev. Mod. Phys. **61**, 605 (1989).
- ¹⁴ R. Stevens, A. Smith, and P. Norris, J. Heat Transfer **127**, 315 (2005).
- ¹⁵ M. E. Lumpkin and W. M. Saslow, Phys. Rev. B. **17**, 4295 (1997).
- ¹⁶ B. V. Paranjape, N. Arimitsu, and E. S. Krebes, J. Appl. Phys. **61**, 888 (1987).
- ¹⁷ D. A. Young and H. J. Maris, Phys. Rev. B. **40**, 3685 (1989).
- ¹⁸ J. Wang and J.-S. Wang, Phys. Rev. B. **74**, 054303 (2006).
- ¹⁹ L. Zhang, J. -S. Wang and B. Li, Phys. Rev. B **78**, 144416 (2008).
- ²⁰ E. Cuansing and J.-S. Wang, Eur. Phys. J. B **69**, 505

- (2009).
- ²¹ J. Velez and W. Butler, *J. Phys.: Condens. Matter* **16**, R637 (2004).
- ²² W. A. Little, *Can. J. Phys.* **37**, 334 (1959).
- ²³ P. E. Hopkins, P. M. Norris, M. S. Tsegaye, and A. W. Glosh, *J. Appl. Phys.* **106**, 063503 (2009).
- ²⁴ M. Schoenberg, *J. Acoust. Soc. Am.* **68**, 1516 (1980).
- ²⁵ A. I. Lavrentyev and S. I. Rokhlin, *J. Acoust. Soc. Am.* **103**, 657 (1998).
- ²⁶ R. Prasher, *Appl. Phys. Lett.* **94**, 041905 (2009).
- ²⁷ M. Hu, P. Keblinski, and P. K. Schelling, *Phys. Rev. B* **79**, 104305 (2009).
- ²⁸ P.A. Khomyakov, G. Brocks, V. Karpan, M. Zwierzycki, P.J. Kelly, *Phys. Rev. B* **72**, 035450 (2005)
- ²⁹ U. Harbola, S. Mukamel, *Phys. Rep.***465**, 191C222 (2008).
- ³⁰ J. -S. Wang, N. Zeng, J. Wang, and C. K. Gan, *Phys. Rev. E* **75**, 061128 (2007)